Published in final edited form as:
Bioorg Med Chem. 2011 March 15; 19(6): 2046–2054. doi:10.1016/j.bmc.2011.01.049.

Development of sulfonamide AKT PH domain inhibitors

Ali Md. Ahad[a], **Song Zuohe**[b], **Lei Du-Cuny**[d], **Sylvestor A. Moses**[c], **Li Li Zhou**[a], **Shuxing Zhang**[d], **Garth Powis**[d], **Emmanuelle J. Meuillet**[b,c], and **Eugene A. Mash**[a,*]

[a] Department of Chemistry and Biochemistry, The University of Arizona, Tucson, Arizona, 85721-0041 USA

[b] Department of Nutritional Sciences, The University of Arizona, Tucson, Arizona, USA

[c] Department of Molecular and Cellular Biology, The University of Arizona, Tucson, Arizona, USA

[d] Department of Experimental Therapeutics, University of Texas, MD Anderson Cancer Center, Houston, Texas, USA

Abstract

Disruption of the phosphatidylinositol 3-kinase/AKT signaling pathway can lead to apoptosis in cancer cells. Previously we identified a lead sulfonamide that selectively bound to the pleckstrin homology (PH) domain of AKT and induced apoptosis when present at low micromolar concentrations. To examine the effects of structural modification, a set of sulfonamides related to the lead compound was designed, synthesized, and tested for binding to the expressed PH domain of AKT using a surface plasmon resonance-based competitive binding assay. Cellular activity was determined by means of an assay for pAKT production and a cell killing assay using BxPC3 cells. The most active compounds in the set are lipophilic and possess an aliphatic chain of the proper length. Results were interpreted with the aid of computational modeling. This paper represents the first structure-activity relationship (SAR) study of a large family of AKT PH domain inhibitors. Information obtained will be used in the design of the next generation of inhibitors of AKT PH domain function.

Keywords

AKT; PH domain; anticancer; drug design; drug development

1. Introduction

Pleckstrin homology (PH) domains containing 100–120 amino acids are found in over 500 human proteins[1] and are the 11th most common domain in the human proteome.[2] A subset of 40 PH domains are known to bind phosphorylated phosphatidylinositol (PI) lipids held in cell membranes. PI phosphorylation and the subsequent binding of PH domain-containing proteins are vital components of signal transduction pathways that regulate cell growth and survival.[3,4] For example, phosphorylation of PI(4,5)P_2 to produce PI(3,4,5)P_3 (see Figure 1)

*Corresponding author. Tel.: +1 520 621 6321; fax +1 520 621 8407. emash@u.arizona.edu.

Supplementary Data
Details of the synthesis and characterization of compounds **1–25** and **41–47** and the associate references.

by PI3K signals the recruitment and binding of AKT to the inner leaflet of the plasma membrane via recognition of the PH domain.[5,6] This translocation allows phosphorylation of AKT at Thr[308] by the plasma membrane-bound PDPK1.[7] Phosphorylation at the Ser[473] residue occurs either by the ILK, by the kinase activity of AKT itself, or by rictor-mTOR.[8] Once fully phosphorylated, AKT translocates through the cytosol to the nucleus where it phosphorylates a variety of downstream targets. AKT promotes cell survival by activating CREB,[9] and promotes proliferation by activating p70S[6] kinase[10] and GSK-3β[11] which contribute to cyclin D accumulation of cell cycle entry. Furthermore, AKT acts as a mediator for VEGF production and angiogenesis by phosphorylation of mTOR.[12] Given its importance in proliferation and survival signaling, AKT is an important target for cancer drug discovery.[13]

Several previous attempts to develop AKT inhibitors have led to compounds that bind to the ATP-binding pocket[14] or behave as allosteric inhibitors.[15] Due to the similarity of this pocket among serine/threonine kinases, achieving target specificity has been difficult. Our previous studies involving a D-3-deoxyphosphatidylinositol ether lipid, DPIEL (Figure 1),[16,17] provided proof-of-principle for using PH domains as drug targets.[17–24] DPIEL exhibits a high binding affinity and selectivity for the PH domain of AKT. In addition, DPIEL does not bind to other PH domain-containing proteins, including PDPK1, IRS-1, mSOS, and βARK. Although DPIEL exhibits significant antitumor activity, unfortunately it is not a useful drug candidate because of its pharmacokinetic and pharmacodynamic properties.[16]

Previously, we used a crystal structure of the PH domain of AKT and *in silico* screening to cull from libraries compounds expected to bind to the target domain.[25,26] Compounds selected from these libraries were purchased or prepared, then tested for binding to AKT and for inhibition of AKT function in several cancer cell lines. Compound **1**, a sulfonamide (see Table 1), was among the leads identified, and so several analogs of **1** were prepared and tested *in vitro*. The best analog, compound **29** herein, was then tested *in vivo* where it exhibited good antitumor activity in a mouse xenograft model of pancreatic cancer cells in immunocompromised mice.[26,27] This work provided for the first time proof-of-principle for further development of sulfonamides as drugs that bind to the PH domain of AKT, inhibit its function, and as a result exhibit antitumor activity. Presented herein are studies with compounds **2**–**47**, derivatives of **1** that were synthesized and tested in an effort to generate structure-activity relationships (SARs) to guide further development of potential drug candidates.

2. Materials and Methods

2.1 Chemical Synthesis

General Experimental—All commercial reagents were used without further purification. Analytical TLC was carried out on pre-coated Silica Gel F254 plates. TLC plates were visualized with UV light (254nm). ^{1}H NMR spectra were recorded at 250, 300, or 500 MHz and ^{13}C NMR spectra at 62.5, 75, or 125 MHz. Chemical shifts (δ) are expressed in ppm and are internally referenced (7.26 ppm for ^{1}H NMR and 77.00 ppm for ^{13}C NMR in $CDCl_3$, 2.50 ppm for ^{1}H NMR and 39.50 ppm for ^{13}C NMR in DMSO-d_6). Mass spectra and high resolution mass spectra were obtained in the Mass Spectrometry Laboratory in the Department of Chemistry at the University of Arizona. Melting points are uncorrected.

4-Butyl-*N*-(1,3,4-thiadiazol-2-yl)benzenesulfonamide (26)—To a solution of butylbenzene (4.13 g, 30.8 mmol) in $CHCl_3$ (50 mL) was added chlorosulfonic acid (17.0 mL, 29.8 g, 256 mmol).[28] The mixture was stirred at rt for 20 h. The mixture was poured on ice (200 mL) and extracted with EtOAc (3 × 100 mL). The combined extracts were washed

with water, aqueous $NaHCO_3$, and water, dried over anhydrous Na_2SO_4, and concentrated in vacuo. The resulting yellow oily residue, crude *p*-butylbenzenesulfonyl chloride (ca 88% yield), was used without further purification in the next reaction; ^{1}H NMR (300 MHz, $CDCl_3$) δ 0.94 (3, t, *J* = 7 Hz), 1.34–1.41 (2, m), 1.62–1.67 (2, m), 2.73 (2, t, *J* = 8 Hz), 7.41 (2, d, *J* = 8 Hz), 7.94 (2, d, *J* = 8 Hz).

To a stirred solution of 2-amino-1,3,4-thiadiazole (2.0 g, 19.7 mmol) in pyridine (30 mL) under argon at −20 °C was added crude *p*-butylbenzenesulfonyl chloride (4.89 g, ca 21 mmol) over 10 min. The reaction mixture was allowed to attain rt and stirred for 16 h. Water (300 mL) was added to quench the reaction. The mixture was extracted with CH_2Cl_2, the organic extracts washed with 2N HCl (2 × 150 mL), brine, dried over anhydrous Na_2SO_4, filtered, and concentrated in vacuo. The residue was subjected to flash chromatography on silica gel eluted with CH_2Cl_2:MeOH 33:1 to give the product **26** (3.46 g, 11.6 mmol, 59% yield) as a solid, mp 120–121 °C; RP HPLC t_R 6.06 min (4.6 × 250 mm C_{18} column eluted with CH_3CN, 0.5 mL/min); ^{1}H NMR (300 MHz, $CDCl_3$) δ 0.91 (3, t, *J* = 7 Hz), 1.29–1.37 (2, m), 1.56–1.61 (2, m), 2.65 (2, t, *J* = 7 Hz), 7.27 (2, d, *J* = 8 Hz), 7.84 (2, d, *J* = 8 Hz), 8.25 (1, s); ^{13}C NMR (75 MHz, $CDCl_3$) 13.9, 22.3, 33.2, 33.6, 126.5, 129.1, 138.1, 142.7, 148.6, 167.4; HRMS (Q-TOF) calculated for $C_{12}H_{16}N_3O_2S_2$ 298.0684, observed 298.0695 $(M+H)^+$; calculated for $C_{12}H_{15}N_3NaO_2S_2$ 320.0503, observed 320.0361 $(M+Na)^+$.

4-Hexyl-*N*-(1,3,4-thiadiazol-2-yl)benzenesulfonamide (27)—In a similar manner, hexylbenzene (5.00 g, 30.8 mmol) and chlorosulfonic acid (17.0 mL, 29.8 g, 256 mmol) gave crude *p*-hexylbenzenesulfonyl chloride as a yellow oily residue (ca 81% yield); ^{1}H NMR (300 MHz, $CDCl_3$) δ 0.88 (3, t, *J* = 7 Hz), 1.30–1.35 (6, m), 1.55–1.63 (2, m), 2.59 (2, t, *J* = 8 Hz), 7.38 (2, d, *J* = 8 Hz), 7.89 (2, d, *J* = 8 Hz). Reaction of 2-amino-1,3,4-thiadiazole (2.0 g, 19.7 mmol) with *p*-hexylbenzenesulfonyl chloride (5.48 g, ca 21 mmol) afforded the product **27** (3.72 g, 11.4 mmol, 58% yield) as a solid, mp 125–126 °C, after flash chromatography on silica gel eluted with CH_2Cl_2:MeOH 33:1; RP HPLC t_R 6.79 min (4.6 × 250 mm C_{18} column eluted with CH_3CN, 0.5 mL/min); ^{1}H NMR (300 MHz, $CDCl_3$) δ 0.88 (3, t, *J* = 7 Hz), 1.28 (6, m), 1.58 (2, m), 2.63 (2, t, *J* = 7 Hz), 7.27 (2, d, *J* = 8 Hz), 7.83 (2, d, *J* = 8 Hz), 8.24 (1, s); ^{13}C NMR (75 MHz, $CDCl_3$) 14.1, 22.6, 28.9, 31.1, 31.6, 35.9, 126.5, 129.0, 138.1, 142.6, 148.6, 167.4; HRMS (Q-TOF) calculated for $C_{14}H_{20}N_3O_2S_2$ 326.0997, observed 326.0931 $(M+H)^+$; calculated for $C_{14}H_{19}N_3NaO_2S_2$ 348.0816, observed 348.0816 $(M+Na)^+$.

4-Octyl-*N*-(1,3,4-thiadiazol-2-yl)benzenesulfonamide (28)—In a similar manner, 1-phenyloctane (5.86 g, 30.8 mmol) and chlorosulfonic acid (17.0 mL, 29.8 g, 256 mmol) gave crude *p*-octylbenzenesulfonyl chloride as a yellow oily residue (ca 80% yield); ^{1}H NMR (300 MHz, $CDCl_3$) δ 0.87 (3, t, *J* = 7 Hz), 1.27–1.32 (10, m), 1.64–1.66 (2, m), 2.72 (2, t, *J* = 8 Hz), 7.42 (2, d, *J* = 8 Hz), 7.93 (2, d, *J* = 8 Hz). Reaction of 2-amino-1,3,4-thiadiazole (2.0 g, 19.7 mmol) with *p*-octylbenzenesulfonyl chloride (6.06 g, ca 21 mmol) afforded the product **28** (3.83 g, 10.8 mmol, 55% yield) as a solid, mp 123–124 °C, after flash chromatography on silica gel eluted with CH_2Cl_2:MeOH 33:1; RP HPLC t_R 8.17 min (4.6 × 250 mm C_{18} column eluted with CH_3CN, 0.5 mL/min); ^{1}H NMR (300 MHz, $CDCl_3$) δ 0.87 (3, t, *J* = 7 Hz), 1.36 (10, m), 1.59 (2, m), 2.63 (2, t, *J* = 7 Hz), 7.27 (2, d, *J* = 8 Hz), 7.82 (2, d, *J* = 8 Hz), 8.23 (1, s); ^{13}C NMR (75 MHz, $CDCl_3$) 14.1, 22.6, 29.2, 29.3, 29.4, 31.1, 31.8, 35.9, 126.5, 129.0, 138.1, 142.6, 148.7, 167.3; HRMS (Q-TOF) calculated for $C_{16}H_{24}N_3O_2S_2$ 354.1310, observed 354.1211 $(M+H)^+$; calculated for $C_{16}H_{23}N_3NaO_2S_2$ 376.1129, observed 376.1154 $(M+Na)^+$.

4-Dodecyl-*N*-(1,3,4-thiadiazol-2-yl)benzenesulfonamide (29)—The syntheses of *p*-dodecylbenzenesulfonyl chloride and compound **29** have previously been described; see the supplementary data associated with reference 26.

4-Tetradecyl-*N*-(1,3,4-thiadiazol-2-yl)benzenesulfonamide (30)—In a similar manner, 1-phenyltetradecane (0.69 g, 2.5 mmol) and chlorosulfonic acid (0.50 mL, 7.5 mmol) gave *p*-tetradecylbenzenesulfonyl chloride as a white solid (0.63 g, 1.7 mmol, 68%), R_f 0.18 (50% EtOAc/hexanes), mp 32–33 °C, after chromatography on silica gel (70–230 mesh) with hexanes/EtOAc (49:1); ^{1}H NMR (300 MHz, $CDCl_3$) δ 0.88 (3, t, *J* = 7.2 Hz), 1.25 (22, m), 1.65 (2, m), 2.72 (2, t, *J* = 7.8 Hz), 7.42 (2, d, *J* = 8.4 Hz), 7.93 (2, d, *J* = 8.4 Hz); ^{13}C NMR (75 MHz, $CDCl_3$) 14.1, 22.6, 29.1, 29.3, 29.5, 29.6, 29.7, 30.9, 31.9, 36.0, 126.9, 129.5, 141.7, 151.6. Reaction of 2-amino-1,3,4-thiadiazole (179 mg, 1.77 mmol) with *p*-tetradecylbenzenesulfonyl chloride (440 mg, 1.18 mmol) afforded the product **30** (240 mg, 0.55 mmol, 47% yield), R_f 0.46 (5% MeOH/CH_2Cl_2), as a solid, mp 116–117 °C, after chromatography on silica gel (70–230 mesh) eluted with CH_2Cl_2:MeOH 19:1; ^{1}H NMR (300 MHz, $CDCl_3$) δ 0.88 (3, t, *J* = 6.9 Hz), 1.25 (22, m), 1.60 (2, m), 2.64 (2, t, *J* = 7.2 Hz), 7.29 (2, d, *J* = 8.4 Hz), 7.84 (2, d, *J* = 8.4Hz), 8.23 (1, s); ^{13}C NMR (75 MHz, $CDCl_3$) 14.1, 22.6, 29.2, 29.3, 29.4, 29.5, 29.6, 31.1, 31.9, 35.9, 126.5, 128.9, 138.1, 142.6, 148.6, 167.4; LRMS (ESI$^+$) calculated for $C_{22}H_{36}N_3O_2S_2$ 438.2, observed 438.3 $(M+H)^+$; HRMS (ESI$^+$, m/z) calculated for $C_{22}H_{36}N_3O_2S_2$ 438.2243, observed 438.2243 $(M+H)^+$.

4-Hexadecyl-*N*-(1,3,4-thiadiazol-2-yl)benzenesulfonamide (31)—In a similar manner, 1-phenylhexadecane (0.76 g, 2.5 mmol) and chlorosulfonic acid (0.50 mL, 7.5 mmol) gave *p*-hexadecylbenzenesulfonyl chloride as a white solid (0.71 g, 1.8 mmol, 72%), mp 35–36 °C, after chromatography on silica gel eluted with hexanes/EtOAc (49:1); ^{1}H NMR (300 MHz, $CDCl_3$) δ 0.88 (3, t, *J* = 7.2 Hz), 1.25 (26, m), 1.62 (2, m), 2.72 (2, t, *J* = 7.8 Hz), 7.42 (2, d, *J* = 8.4 Hz), 7.95 (2, d, *J* = 8.4 Hz); ^{13}C NMR (75 MHz, $CDCl_3$) 14.4, 22.9, 29.4, 29.64, 29.8, 29.9, 31.2, 32.2, 36.3, 127.3, 129.8, 142.0, 151.9. Reaction of 2-amino-1,3,4-thiadiazole (228 mg, 2.25 mmol) with *p*-hexadecylbenzenesulfonyl chloride (600 mg, 1.50 mmol) afforded the product **31** (320 mg, 0.69 mmol, 46% yield), R_f 0.46 (5% MeOH/CH_2Cl_2), as a solid, mp 118–119 °C, after chromatography on silica gel (70–230 mesh) eluted with CH_2Cl_2:MeOH 19:1; ^{1}H NMR (300 MHz, $CDCl_3$) δ 0.88 (3, t, *J* = 6.9 Hz), 1.25 (26, m), 1.59 (2, m), 2.64 (2, t, *J* = 8.1 Hz), 7.29 (2, d, *J* = 7.8 Hz), 7.84 (2, d, *J* = 7.8 Hz), 8.23 (1, s); ^{13}C NMR (75 MHz, $CDCl_3$) 14.1, 22.7, 29.2, 29.3, 29.4, 29.6, 29.7, 31.1, 31.9, 35.9, 126.5, 128.9, 138.1, 142.5, 148.7, 167.5; LRMS (ESI$^+$) calculated for $C_{24}H_{40}N_3O_2S_2$ 466.3, observed 466.3 $(M+H)^+$; HRMS (ESI$^+$, m/z) calculated for $C_{24}H_{40}N_3O_2S_2$ 466.2556, observed 466.2558 $(M+H)^+$.

4-Octadecyl-*N*-(1,3,4-thiadiazol-2-yl)benzenesulfonamide (32)—In a similar manner, 1-phenyloctadecane (0.84 g, 2.5 mmol) and chlorosulfonic acid (0.50 mL, 7.5 mmol) gave *p*-octadecylbenzenesulfonyl chloride as a white solid (0.60 g, 1.4 mmol, 56%), mp 43–44 °C, after chromatography on silica gel eluted with hexanes/EtOAc (49:1); ^{1}H NMR (300 MHz, $CDCl_3$) δ 0.86 (3, t, *J* = 6.9 Hz), 1.25 (30, m), 1.65 (2, m), 2.72 (2, t, *J* = 7.8 Hz), 7.42 (2, d, *J* = 8.4 Hz), 7.93 (2, d, *J* = 8.4 Hz); ^{13}C NMR (75 MHz, $CDCl_3$) 14.1, 22.7, 29.2, 29.4, 29.5, 29.7, 30.9, 31.9, 36.0, 127.1, 129.6, 141.8, 151.7. Reaction of 2-amino-1,3,4-thiadiazole (177 mg, 1.75 mmol) with *p*-octadecylbenzenesulfonyl chloride (500 mg, 1.17 mmol) afforded the product **32** (296 mg, 0.60 mmol, 51% yield), R_f 0.46 (5% MeOH/CH_2Cl_2), as a solid, mp 116–117 °C, after chromatography on silica gel (70–230 mesh) eluted with CH_2Cl_2:MeOH 19:1; ^{1}H NMR (300 MHz, $CDCl_3$) δ 0.86 (3, t, *J* = 6.9 Hz), 1.25 (30, m), 1.60 (2, m), 2.64 (2, t, *J* = 7.8 Hz), 7.29 (2, d, *J* = 7.8 Hz), 7.82 (2, d, *J* = 7.8 Hz), 8.21 (1, s); ^{13}C NMR (75 MHz, $CDCl_3$) 14.0, 22.7, 29.2, 29.3, 29.4, 29.5, 29.6, 29.7, 31.1, 31.9, 35.9, 126.5, 128.9, 138.1, 142.6, 148.6, 167.4; LRMS (ESI$^+$) calculated for $C_{26}H_{44}N_3O_2S_2$ 494.3, observed 494.2 $(M+H)^+$; HRMS (ESI$^+$, m/z) calculated for $C_{26}H_{44}N_3O_2S_2$ 494.2869, observed 494.2869 $(M+H)^+$.

4-Dodecyl-*N*-(5-methyl-1,3,4-thiadiazol-2-yl)benzenesulfonamide (33)—A suspension of 2-amino-5-methyl-1,3,4-thiadiazole (150 mg, 1.3 mmol) in pyridine (0.5 mL) was stirred and cooled in an ice bath while *p*-dodecylbenzenesulfonyl chloride (300 mg, 0.87 mmol) was added slowly. The reaction mixture was allowed to attain rt, then heated in an oil bath at 95 °C for 1 h. The reaction mixture was then cooled, added to aqueous 10% HCl (5 mL), and the resulting mixture extracted with EtOAc (3 × 10 mL). The organic extracts were washed with water, brine, dried over anhydrous Na_2SO_4, filtered, and volatiles evaporated in vacuo to yield a solid mass. Chromatography on silica gel (70–230 mesh) eluted with CH_2Cl_2:MeOH 49:1 gave the product **33** (310 mg, 0.73 mmol, 84%), R_f 0.23 (50% EtOAc/hexanes). Recrystallization from EtOAc:hexanes 7:3 gave an analytical sample, mp 149–150 °C; ^{1}H NMR (500 MHz, $CDCl_3$) δ 0.88 (3, t, *J* = 7.0 Hz), 1.20–1.36 (18, m), 1.54–1.63 (2, m), 2.51 (3, s), 2.63 (2, t, *J* = 7.5 Hz), 7.25 (2, d, *J* = 7.5 Hz), 7.82 (2, d, *J* = 7.5 Hz), 12.36 (1, br s); ^{13}C NMR (125 MHz, $CDCl_3$) δ 14.1, 16.5, 22.7, 29.2, 29.3, 29.4, 29.5, 29.6, 31.1, 31.9, 35.9, 126.4, 128.8, 138.3, 148.3, 154.1, 168.6; LRMS (ESI^+, m/z) calculated for $C_{21}H_{34}N_3O_2S_2$ 424.2092 observed 424.20 $(M+H)^+$; HRMS (ESI^+, m/z) calculated for $C_{21}H_{34}N_3O_2S_2$ 424.2092, observed 424.2085 $(M + H)^+$.

4-Dodecyl-*N*-(5-ethyl-1,3,4-thiadiazol-2-yl)benzenesulfonamide (34)—In a similar manner, reaction of 2-amino-5-ethyl-1,3,4-thiadiazole (169 mg, 1.3 mmol) and *p*-dodecylbenzenesulfonyl chloride (300 mg, 0.87 mmol) gave the product **34** (225 mg, 0.51 mmol, 59%), R_f 0.27 (50% EtOAc/hexanes), after chromatography on silica gel (70–230 mesh) eluted with CH_2Cl_2:MeOH 49:1. Recrystallization from EtOAc:hexanes 7:3 gave an analytical sample, mp 93–94 °C; ^{1}H NMR (500 MHz, $CDCl_3$) δ 0.88 (3, t, *J* = 6.5 Hz), 1.20–1.36 (18, m), 1.33 (3, t, *J* = 7.5 Hz), 1.54–1.63 (2, m), 2.63 (2, t, *J* = 7.5 Hz), 2.84 (2, q, *J* = 7.5 Hz), 7.25 (2, d, *J* = 8.5 Hz), 7.83 (2, d, *J* = 8.5 Hz), 12.30 (1, br s); ^{13}C NMR (125 MHz, $CDCl_3$) δ 12.6, 14.1, 22.7, 24.4, 29.2, 29.3, 29.4, 29.5, 29.6, 31.1, 31.9, 35.9, 126.5, 128.8, 138.4, 148.2, 160.1 168.2; LRMS (ESI^+, m/z) calculated for $C_{22}H_{36}N_3O_2S_2$ 438.2249, observed 438.30 $(M+H)^+$; HRMS (ESI^+, m/z) calculated for $C_{22}H_{36}N_3O_2S_2$ 438.2249, observed 438.2247 $(M + H)^+$.

***N*-(5-*tert*-Butyl-1,3,4-thiadiazol-2-yl)-4-dodecylbenzenesulfonamide (35)—**In a similar manner, reaction of 2-amino-5-*tert*-butyl-1,3,4-thiadiazole (204 mg, 1.3 mmol) and *p*-dodecylbenzenesulfonyl chloride (300 mg, 0.87 mmol) gave the product **35** (350 mg, 0.75 mmol, 86%), R_f 0.45 (50% EtOAc/hexanes), after chromatography on silica gel (70–230 mesh) eluted with CH_2Cl_2:MeOH 49:1. Recrystallization from EtOAc:hexanes 7:3 gave an analytical sample, mp 117–118 °C; ^{1}H NMR (500 MHz, $CDCl_3$) δ 0.88 (3, t, *J* = 6.5 Hz), 1.20–1.36 (18, m), 1.38 (9, s), 1.56–1.64 (2, m), 2.63 (2, t, *J* = 7.5 Hz), 7.25 (2, d, *J* = 8.0 Hz), 7.86 (2, d, *J* = 8.0 Hz), 12.24 (1, br s); ^{13}C NMR (125 MHz, $CDCl_3$) δ 14.1, 22.7, 29.2, 29.3, 29.4, 29.5, 29.6, 29.7, 31.1, 31.8, 35.8, 36.5, 126.5, 128.7, 138.5, 148.1, 167.8, 168.0; LRMS (ESI^+, m/z) calculated for $C_{24}H_{40}N_3O_2S_2$ 466.3, observed 466.2 $(M+H)^+$; HRMS (ESI^+, m/z) calculated for $C_{24}H_{40}N_3O_2S_2$ 466.2562, observed 466.2562 $(M + H)^+$.

2-(5-(4-Dodecylphenylsulfonamido)-1,3,4-thiadiazol-2-yl)acetic Acid (36)—Distilled water (3.0 mL) and 10% aqueous NaOH (0.65 mL) were added to compound **37** (200 mg, 0.40 mmol) and the mixture was heated under reflux for 2 h. The pH of the solution was then adjusted to 4.0 by addition of 1.0 M HCl, the resulting precipitate was isolated by filtration, washed with cold water, and dried to give the product **36** (161 mg, 0.34 mmol, 85%), R_f 0.34 (20% MeOH/CH_2Cl_2), as a light yellow solid, mp 194–195 °C; ^{1}H NMR (300 MHz, DMSO-d_6) δ 0.85 (3, t, *J* = 6.6 Hz), 1.23 (18, m), 1.53 (2, m), 2.57 (2, t, *J* = 7.5 Hz), 3.74 (2, s), 7.24 (2, d, *J* = 8.1 Hz), 7.61 (2, d, *J* = 7.8 Hz); ^{13}C NMR (75 MHz, DMSO-d_6) δ 14.0, 22.1, 28.8, 28.9, 29.1, 30.7, 31.3, 34.9, 37.4, 125.8,128.4, 141.2, 146.0, 153.3, 168.9, 170.8; LRMS (ESI^+) calculated for $C_{22}H_{34}N_3O_4S_2$ 468.2, observed

468.2 $(M+H)^+$; HRMS (ESI^+, m/z) calculated for $C_{22}H_{34}N_3O_4S_2$ 468.1991, observed 468.1977 $(M+H)^+$.

Ethyl 2-(5-(4-Dodecylphenylsulfonamido)-1,3,4-thiadiazol-2-yl)acetate (37)—A suspension of ethyl 2-(5-amino-1,3,4-thiadiazol-2-yl)acetate[29] (2.0 g, 11.2 mmol) in pyridine (50 mL) was stirred and cooled in an ice bath while *p*-dodecylbenzenesulfonyl chloride (4.7 g, 13.5 mmol) was added slowly. The mixture was stirred at rt for 48 h, then heated in an oil bath at 90 °C for 15 min. The reaction mixture was then cooled to rt, poured into aqueous 10% HCl, and extracted with EtOAc (3 × 75 mL). The combined extracts were washed with water (2 × 50 mL), brine (2 × 50 mL), dried over anhydrous Na_2SO_4, filtered, and concentrated in vacuo. The residue was subjected to chromatography on silica gel (70–230 mesh) eluted with CH_2Cl_2:MeOH 95:5 to give the product **37** (2.9 g, 5.9 mmol, 53%), R_f 0.64 (10% MeOH/CH_2Cl_2). Recrystallization from EtOAc/hexanes gave an analytical sample, mp 110–111 °C; ^{1}H NMR (500 MHz, $CDCl_3$) δ 0.88 (3, t, *J* = 7.0 Hz), 1.20–1.28 (18, m), 1.32 (3, t, *J* = 7.0 Hz), 1.58–1.66 (2, m), 2.64 (2, t, *J* = 7.0 Hz), 3.87 (2, s), 4.25 (2, q, *J* = 7.0 Hz), 7.26 (2, d, *J* = 8.0 Hz), 7.82 (2, d, *J* = 8.0 Hz), 10.91 (1, br s); ^{13}C NMR (125 MHz, $CDCl_3$) δ 14.0, 14.1, 22.6, 29.2, 29.3, 29.4, 29.5, 29.6, 31.1, 31.9, 35.9, 36.4, 62.2, 126.4, 128.8, 138.2, 148.3, 151.2, 167.3, 168.6; LRMS (ESI^+) calculated for $C_{24}H_{38}N_3O_4S_3$ 496.2, observed 496.2 $(M+H)^+$; HRMS (ESI^+, m/z) calculated for $C_{24}H_{38}N_3O_4S_3$ 496.2304, observed 496.2295 $(M+H)^+$.

Ethyl 5-(4-Dodecylphenylsulfonamido)-1,3,4-thiadiazol-2-carboxylate (38)—In a similar manner, reaction of ethyl 5-amino-1,3,4-thiadiazole-2-carboxylate[30] (1.8 g, 10.4 mmol) with *p*-dodecylbenzenesulfonyl chloride (4.3 g, 12.5 mmol) gave the product **38** (3.9 g, 8.1 mmol, 78%), R_f 0.44 (10% MeOH/CH_2Cl_2), after chromatography on silica gel (70–230 mesh) eluted with CH_2Cl_2:MeOH 9:1. Recrystallization from EtOAc/hexanes gave an analytical sample, mp 134–135 °C; ^{1}H NMR (600 MHz, DMSO-d_6) δ 0.84 (3, t, *J* = 7.0 Hz), 1.17–1.30 (18, m), 1.31 (3, t, *J* = 7.0 Hz), 1.50–1.51 (2, m), 2.62 (2, t, *J* = 7.0 Hz), 4.36 (2, q, *J* = 7.0 Hz), 7.38 (2, d, *J* = 8.0 Hz), 7.72 (2, d, *J* = 8.0 Hz); ^{13}C NMR (150 MHz, DMSO-d_6) δ 14.3, 22.6, 29.1, 29.2, 29.3, 29.4, 29.5, 31.1, 31.8, 35.4, 63.4, 126.4, 129.4, 139.1, 147.7, 148.3, 157.9, 168.1; LRMS (ESI^+) calculated for $C_{23}H_{36}N_3O_4S_3$ 482.2, observed 482.1 $(M+H)^+$; HRMS (ESI^+, m/z) calculated for $C_{23}H_{36}N_3O_4S_3$ 482.2140, observed 482.2134 $(M+H)^+$.

4-Dodecyl-N-(5-(hydroxymethyl)-1,3,4-thiadiazol-2-yl)benzenesulfonamide (39)—In a similar manner, reaction of 2-amino-5-hydroxymethyl-1,3,4-thiadiazole[31] (4.0 g, 30.5 mmol) with *p*-dodecylbenzenesulfonyl chloride (11.6 g, 33.6 mmol) gave the product **39** (8.7 g, 19.8 mmol, 65% yield), R_f 0.58 (10% MeOH/CH_2Cl_2), as a solid, mp 138–139 °C, after chromatography on silica gel (70–230 mesh) eluted with CH_2Cl_2:MeOH 19:1; ^{1}H NMR (300 MHz, DMSO-d_6) δ 0.84 (3, t, *J* = 6.6 Hz), 1.22 (18, m), 1.54–1.57 (2, m), 2.64 (2, t, *J* = 7.8 Hz), 4.57 (2, s), 6.05 (1, br s), 7.35 (2, d, *J* = 8.1 Hz), 7.67 (2, d, *J* = 7.8 Hz); ^{13}C NMR (75 MHz, DMSO-d_6) δ 13.9, 22.1, 28.6, 28.7, 28.8, 29.0, 30.6, 31.3, 34.9, 58.4, 125.8, 128.9, 139.2, 147.5, 161.1, 167.5; LRMS (ESI^+) calculated for $C_{21}H_{34}N_3O_3S_2$ 440.2, observed 440.2 $(M+H)^+$; HRMS (ESI^+, m/z) calculated for $C_{21}H_{34}N_3O_3S_2$ 440.2042, observed 440.2029 $(M+H)^+$.

5-(4-Dodecylphenylsulfonamido)-1,3,4-thiadiazole-2-sulfonamide (40)—A suspension of 5-amino-1,3,4-thiadiazolo-2-sulfonamide[32] (4.10 g, 22.8 mmol) in anhydrous acetonitrile (100 mL) was stirred and cooled in an ice bath. Triethylamine (2.5 g, 25 mmol) and a solution of *p*-dodecylbenzenesulfonyl chloride (8.6 g, 25 mmol) in anhydrous acetonitrile (60 mL) were added, the reaction mixture allowed to attain rt, and then stirred for 48 h. Volatiles were removed *in vacuo* and the residue was washed with 10% aqueous

HCl (100 mL) and water (100 mL) in order to eliminate salts. The residue was subjected to chromatography on silica gel (70–230 mesh) eluted with CH_2Cl_2:MeOH 19:1 to give the product **40** (7.0 g, 14.3 mmol, 63%), R_f 0.56 (10% MeOH/CH_2Cl_2). Recrystallization from absolute ethanol and a second chromatography gave an analytical sample, mp 249–250 °C; ^{1}H NMR (300 MHz, DMSO-d_6) δ 0.85 (3, t, J = 6.6 Hz), 1.23 (18, m), 1.55 (2, m), 2.58 (2, t, J = 7.2 Hz), 7.23 (2, d, J = 7.8 Hz), 7.34 (2, s), 7.59 (2, d, J = 8.1 Hz); ^{13}C NMR (75 MHz, DMSO-d_6) δ 13.9, 22.1, 28.7, 28.9, 29.0, 29.1, 30.8, 31.3, 34.9, 126.2, 127.8, 143.3, 145.1, 161.2, 170.9; LRMS (ESI$^-$) calculated for $C_{20}H_{31}N_4O_4S_3$ 487.2, observed 487.1 (M-H)$^-$; HRMS (ESI$^-$, m/z) calculated for $C_{20}H_{31}N_4O_4S_3$ 487.1513, observed 487.1514 (M-H)$^-$.

2.2 Biological studies

2.2.1 Expression of recombinant AKT PH domain—Recombinant mouse AKT1 PH domain amino acids 1–111 (UBI/Millipore, Charlottesville, VA) was cloned by PCR into EcoRI/XhoI sites in pGEX-4T1 inducible bacterial expression plasmid (GeneStorm, InVitrogen, Carlsbad, CA) transformed into BL21(DE3) *E. Coli*. Expression and purification of the protein were performed as previously described.[15]

2.2.2 Surface plasmon resonance (SPR) spectroscopy binding assays—Competitive binding assays were performed with a Biacore 2000, using the Biacore 2000 Control Software v3.2 and BIAevaluation v4.1 analysis software (Biacore, Piscataway, NJ) as previously described.[26] Briefly, PI-3,4,5-phosphates-biotin labeled liposomes (Echelon Biosciences, Salt Lake City, UT) were immobilized on SA chips (BR-1000-32) at a level of 600 response units (RUs). Small molecule analytes at concentrations ranging from one tenth to ten times the predicted K_D were co-injected with 80nM PH domain GST-fusion protein (AKT1) at a flow rate of 30uL/min. Dimethylsulfoxide (DMSO) concentrations in all samples and running buffer were 1% (v/v) or less.

2.2.3 Cell assays

Cellular proliferation: A standard 96-well micro-cytoxicity assay was performed by plating cells at 5,000–10,000 cells per well (depending on cell doubling time) for a growth period of 4 days. Drugs were added directly to the media, dissolved in DMSO at various concentrations ranging from 1 to 50 μM. The endpoint was spectrophotometric determination of the reduction of 3-(4,5-dimethylthiazol-2-yl)-2,5-diphenyltetrazolium bromide.

Detection of pAKT: Human BxPC3 pancreatic cancer cells were obtained from the American Type Culture Collection (Rockville, MD). Cells were maintained in bulk culture in Dulbecco's modified Eagle medium (DMEM) supplemented with 10% heat-inactivated fetal bovine serum (FBS), 4.5 g/L glucose, 100 U/mL penicillin and 100 μg/mL streptomycin in a 5% CO_2 atmosphere. Cells were passaged using 0.25% trypsin and 0.02% EDTA. Cells were confirmed to be mycoplasma free by testing them with an ELISA kit (Roche-Boehringer Mannheim, Indianapolis, IN). Drugs were freshly prepared in DMSO at a stock concentration of 10 mM and then added at 10μM final concentration directly into the culture media of the cells for 4 h. Following this treatment, cells were lysed as previously published[26] and equal amounts of total cell lysate were loaded on a pSer^{473}-AKT/Total AKT Meso Scale Discovery plate. The plate was read using a Sector Imager 2400A instrument (Meso Scale Discovery protein profiling system, Gaithersburg, MD).

2.3 Computational modeling

In a previous study[33] GOLD docking and scoring[34] was reported as the best combination for the analysis of interactions between the AKT PH domain and small molecules. Therefore, the GOLD package was employed for molecular docking studies in this work. During docking, the protein was kept as rigid while the flexibility of the ligand was explored. Flipping of the ring corners in the ligands was considered, and carboxylic acids were deprotonated. No early termination was allowed in docking. Other parameters and procedures were applied as previously described.[33]

3. Results

3.1 Chemistry

The structures, yields, and melting points of compounds **1–47** are given in Table 1. Compounds **1–4** and **8–10** are listed as being commercially available, but only **2** is inexpensive. Compounds **1–5**, **7–10**, and **16** are known and were prepared for this study according to literature procedures. Most of the remaining compounds were prepared by condensation of a 2-amino-1,3,4-thiadiazole nucleophile with an arenesulfonyl chloride electrophile in the presence of pyridine. The 2-amino-1,3,4-thiadiazoles and arenesulfonyl chlorides used were either obtained from commercial sources or were prepared by known methods. Yields of these condensations were generally good to excellent. In some cases, substituent modification followed condensation to produce additional analogs (e.g., saponification of esters **13**, **22**, and **37** gave acids **12**, **21**, and **36**, respectively). Compounds were purified by column chromatography and/or crystallization. Structures were confirmed by spectroscopic methods and purity ascertained to be ≥95% by TLC analysis or by RP HPLC analysis. Details of the syntheses and compound characterization for compounds **26–40** are given in the Experimental Section. Details of the syntheses and compound characterization data for compounds **1–25** and **41–47** are given in the Supplementary Data that accompanies this paper.

3.2 Bioassays

Results from bioassays of compounds **1–47** are given in Table 2 and Figure 2. Compounds were tested for their ability to compete with the binding of PI(3,4,5)P_3 to the PH domain of AKT (reported as K_i) using a previously described surface plasmon resonance (SPR) competitive binding assay.[26,27] Compounds **1** and **8** that bear hydrogen atoms at positions R_1, R_2, and R_3 and an amino or acetamido substituent at position R_4, respectively, exhibited no ability to block PI(3,4,5)P_3 binding (K_i > 50 μM). As a result, K_i values for compounds **2–7** and **9–16** were not determined. Compounds **17–24** that bear hydrogen atoms at positions R_2 and R_3 and a decamido substituent at position R_4, but vary at R_1, were shown to compete with the binding of PI(3,4,5)P_3 with most K_i values near 10 μM. Replacement of the hydrophobic decamido substituent of **17** with a more hydrophilic PEG-containing amide in **44** reduced inhibition of PI(3,4,5)P_3 binding. Compounds **26–32** bear hydrogen atoms at positions R_1, R_2, and R_3 and a normal alkyl substituent of variable length at position R_4. As previously reported, an aliphatic chain of the proper length (~$C_{12}H_{25}$) is necessary for optimal inhibition of PI(3,4,5)P_3 binding.[27] The K_i values for compounds **33–40** that bear hydrogen atoms at positions R_2 and R_3, a $C_{12}H_{25}$ substituent at position R_4, and an additional substituent (R_1) at position 5 of the thiadiazole ring were unimproved relative to **29**. Replacement of the $C_{12}H_{25}$ chain at R_4 with a phenyl (compare **29** with **41**, **34** with **42**, and **39** with **43**) or replacement of the thiadiazole ring with a phenyl (compare **29** with **45**) was detrimental to inhibition of PI(3,4,5)P_3 binding. Movement of the $C_{12}H_{25}$ chain from the *para* position to the *ortho* or *meta* position relative to the sulfonamide (compare **29** with **46** and **47**) also reduced inhibition of PI(3,4,5)P_3 binding.

Following binding experiments, cellular assays were conducted: cellular proliferation (see Table 2, IC_{50} values) and inhibition of AKT activation in BxPC3 cells (Figure 2) were measured in the presence of compounds **1–47**. Cellular activity tracks reasonably well with the K_i values. Compounds **1–16** with an amino or acetamido substituent at R_4 were inactive. Several compounds bearing a decanamido substituent at R_4 showed some activity in one or both assays (e.g., **17**, **19**, **20**, and **23**). The best activities were exhibited by compounds **29**, **30**, **33–35**, and **37** that possess $C_{12}H_{25}$ or $C_{14}H_{29}$ substituents at R_4 and in some cases an R_1 substituent at position 5 of the thiadiazole ring. Replacement of the R_4 alkyl substituent by phenyl or a PEG amide gave inactive compounds **41–44**. Interestingly, compound **45**, with a phenyl substituent in place of the thiadiazole ring, did not inhibit phosphorylation of AKT at Ser^{473} but did inhibit BxPC-3 cell proliferation. The position of the aliphatic chain also mattered, as compounds **46** and **47** with dodecyl groups *ortho* and *meta* to the sulfonamide did not greatly inhibit the production of pAKT but did inhibit BxPC-3 cell proliferation.

3.3 Computational Modeling

Molecular docking was used to investigate the binding of compounds **1–47** to the AKT PH domain. The best docking pose of each compound was selected according to the GOLD docking scores, the populations of the pose clusters, and their interactions with the binding pocket. For the purposes of this discussion, compounds **1, 17, 29,** and **37** were selected to represent molecules in different chemical subgroups based on the substituent present at position R_4. The best docking poses of these four molecules and of inositol(1,3,4,5)tetraphosphate (IP_4) with the AKT PH domain are illustrated in Figure 3. In each case, the sulfonamide group interacts with Arg23, Arg25, and Lys14 in a manner similar to the best pose exhibited by compound **1**.[28] Compounds **2–7** and **8–16** bear amino and acetamido groups at R_4, respectively, and variable substitution at R_1. For the most part, these modifications did not result in large changes in the GOLD docking scores (see Table 2). Increasing the length of the carboxamide chain at R_4 by replacement of the acetamido group with a decanamido group, as in compounds **17–25**, improved the GOLD docking scores by an average of 7. This is consistent with the greater activity of these compounds as evidenced by the measured K_i values (Table 2).

Compound **29** is representative of the set of compounds **26–32** that possess alkyl substituents of varying length at R_4. As depicted in Figure 3, the nitrogen atoms of the thiadiazole ring of **29** form hydrogen bonds with residue Glu17. The dodecyl chain extends from the main binding pocket to the protein surface, where it appears to interact with the hydrophobic residue Phe55. Shorter chains, as in **26**, do not reach Phe55, thus weakening the binding. Based on our docking studies, the presence of a too-long chain, as in **31** and **32**, changes the binding pose of the thiadiazole and sulfonamide moieties (not depicted). Compounds **29** and **30** that possess alkyl chains of optimal length ($C_{12}H_{25}$ and $C_{14}H_{29}$, respectively) exhibit stronger binding, as suggested by GOLD docking scores and confirmed by experimental observations (see Table 2).

As with **29**, compounds **33–40** bear an optimal $C_{12}H_{25}$ chain at R_4, and in addition, a substituent R_1 on the thiadiazole ring. The R_1 substituents range from nonpolar alkyl groups that vary in size, to more polar substituents containing carboxylic acid, carboxylate ester, and sulfonamide groups. The more polar groups were expected to mimic the phosphate at C-1 of PI(3,4,5)P_3 and possibly interact with Arg23. Most of the compounds in this series exhibited relatively high GOLD docking scores (60–70) as well as measurable to good K_i values in an SPR-based competitive binding assay. For example, compounds **36** and **37**, which bear carboxymethyl and 2-ethoxy-2-oxoethyl substituents at R_1, possess two of the three highest GOLD docking scores obtained and K_i values of 5.0 and 4.3 μM, respectively, indicative of relatively strong competitive binding against PI(3,4,5)P_3. The best binding poses of these compounds exhibit protein-small molecule interactions similar to those of **29**

and also interact with Arg23 via the carbonyl moiety of the R_1 substituent. The ethoxy group of **37** also exhibits hydrophobic interactions with Tyr18 and Ile19.

Structural modifications as in compounds **41–45** were detrimental to binding. Movement of the $C_{12}H_{25}$ chain from the *para* position (compound **29**) to the *ortho* (**46**) or *meta* (**47**) positions also decreased the GOLD docking scores and experimentally measured K_i values.

In order to improve our inhibitor design capabilities, the flexibility of the PH domain is under study using molecular dynamics and normal mode analysis.[36] By examining both backbone and side chain flexibility, we have found that docking predictions using the apo-structure produced results similar to those using more complex structures. In the present case of the AKT PH domain, 12 ns molecular dynamics following rigid docking demonstrated that accounting for protein flexibility did not improve the docking results significantly. The compound **29**-PH domain complex was relatively stable, more or less staying bound in the original docked conformation except for the very end of the alkyl tail (see Supplementary Data for a dynamics movie). This suggests our approach to docking ligands into a rigid AKT PH domain structure virtual screening for targets for which complex crystal structures are unavailable has validity, in particular for this series of compounds related to **29**.[37]

The availability of the crystal structure of the AKT kinase-PH domain with allosteric inhibitors provides additional understanding of this system.[38] Structural alignment with the IP4-PH domain complex indicates that only the far side of loop 3–4 showed a significant difference and the kinase domain disrupts the phospholipid binding site of the PH domain (Figure 4). Therefore our inhibitors will not bind to this state of the PH domain.

4. Discussion

In recent years, we identified a family of sulfonamides as being AKT inhibitors based on their direct binding to the PH domain and their cellular and in vivo activities.[16, 25–27] Although there have been other efforts to develop AKT PH domain inhibitors, few SAR studies based on lead compounds and few studies where antitumor properties have been demonstrated in animals have appeared.[18, 23, 39–42] The present study represents the first large SAR study on sulfonamide AKT PH domain inhibitors.

Based on docking of **1** to the PH domain of AKT, analogs **2–47** were designed, synthesized, tested for binding using an SPR-based assay, and for cellular activity. Modeling suggested that modification at position R_4 would not disturb the best binding mode of **1** since R_4 points away from the PI(3,4,5)P_3 binding pocket (Figure 3). Compounds with small groups at R_4, including **1–7** (R_1 variable, $R_2 = R_3 = H$, $R_4 = NH_2$), **8–16** (R_1 variable, $R_2 = R_3 = H$, R_4 = acetamido), and **26–28** ($R_1 = R_2 = R_3 = H$, $R_4 = C_4$-C_8 alkyl chain) do not bind significantly to the AKT PH domain as determined by SPR measurements of competitive binding against PI(3,4,5)P_3. Some compounds with longer amide-derived substituents at R_4 (decanamides **17–24** and PEG-amide **44**) exhibited the ability to inhibit PI(3,4,5)P_3 binding ($K_i < 50$ μM), but at best weak cellular activity. SAR analysis also suggested that compounds with an aliphatic chain of the appropriate length at R_4 (e.g., **29** and **30**) exhibited the ability to inhibit PI(3,4,5)P_3 binding (K_i) and good cellular activity as measured by inhibition of AKT phosphorylation and a cell survival assay using BxPC3 cells. However, the need to employ both binding and *in vitro* assays was underscored by the observation that compounds **31** and **32** bearing $C_{16}H_{33}$ and $C_{18}H_{37}$ chains, respectively, at R_4, exhibited low μM values of K_i and the lowest IC_{50} values in the cell survival assay, but had little effect on AKT activity, as measured by the pAKT/AKT ratio. In addition, replacement of the thiadiazole ring of **29** with a phenyl ring (compound **45**) decreased the K_i value, and **45** did not inhibit the

production of pAKT, but did inhibit BxPC-3 cell proliferation. These observations suggest that cell-based activities depend not only on binding affinity, but also on other properties, such as cell permeability and compound solubility. In addition, off-target effects may occur and confound interpretation of the results. Off target effects of phosphatidylinositol ether lipid analogs (PIAs) led to the discovery that such compounds can activate a single isoform of p38, p38α, *in vitro* and *in vivo*.[43] It was concluded that because p38α activation occurs in cancer cells after chemotherapy and in normal cells during inflammatory processes, activation of p38α by PIAs could contribute to the efficacy and/or toxicity of PIAs.

Modeling also suggested that the sulfonamide moieties of strongly bound compounds, such as **29**, mimic the phosphate group at C-3 of PI(3,4,5)P_3 by interacting with Arg23, Arg25, and Lys14 (see Figure 3). As PI(3,4,5)P_3 also interacts with Tyr18, Ile19, and Arg86 through the C-1 phosphate, substituents were introduced at position R_1 to mimic the C-1 phosphate. Compounds **18–25**, **33–40**, and **42–43** were of most interest in this regard, but exhibited K_i and IC_{50} values similar to those of the reference compounds bearing H at R_1 (**17**, **29**, and **41**, respectively). Thus, substitution at R_1 appears to be of lesser importance than was expected.

Although studies have shown that most of the current scoring functions in docking are of limited accuracy and the docking scores usually are not well correlated with experimentally measured binding affinities,[35] in the present study a correlation between the GOLD docking scores and p*K*i (see Table 2) is apparent (Figure 5). Docking suggested that the two outliers, compounds **31** and **32**, adopt alternate binding poses due to the steric problems caused by the too-long alkyl chains. This agreement between the GOLD docking scores and the experimentally determined pK_i values supports our previous assertion that the combination of GOLD docking and GOLD scoring is appropriate for modeling this system.[33]

Supplementary Material

Refer to Web version on PubMed Central for supplementary material.

Acknowledgments

This work was supported by grants RO1 CA 061015 and P30 CA 23074 from the National Cancer Institute. SM was supported in part by the MGE@MSA fellowship and by the Alfred P. Sloan Foundation.

Abbreviations

AKT	protein kinase B
β-ARK	beta-adrenergic receptor kinase
CREB	cAMP response element-binding
DMEM	Dulbecco’s modified Eagle medium
DPIEL	deoxyphosphatidylinositol ether lipid
ELISA	enzyme-linked immunosorbent assay
ESI	electrospray ionization
FBS	fetal bovine serum
HRMS	high resolution mass spectrum
ILK	integrin-linked kinase
IRS-1	insulin receptor substrate-1

LRMS	low resolution mass spectrum
mSOS	mammalian son-of-sevenless
mTOR	mammalian target of rapamycin
PDPK1	3-phosphoinositide dependent protein kinase-1
PH	pleckstrin homology
PI	phosphoinositol
PI3K	phosphatidylinositol 3-kinase
PI(4	5)P_2, phosphatidylinositol (4,5)-bisphosphate
PI(3	4,5)P_3, phosphatidylinositol (3,4,5)-trisphosphate
RP HPLC	reversed phase high performance liquid chromatography
SAR	structure-activity relationship
TLC	thin-layer chromatography
VEGF	vascular endothelial growth factor

References and notes

1. Rebecchi MJ, Scarlata S. Ann Rev Biophys Biomol Struct. 1998; 27:503. [PubMed: 9646876]
2. Lemmon MA. Biochem Soc Symp. 2007; 74:81. [PubMed: 17233582]
3. Park WS, Heo WD, Whalen JH, O'Rourke NA, Bryan HM, Meyer T, Teruel MN. MolCell. 2008; 30:381.
4. Nicholson KM, Anderson NG. Cell Signal. 2002; 14:381. [PubMed: 11882383]
5. Zhao L, Vogt PK. Oncogene. 2008; 27:5486. [PubMed: 18794883]
6. Scheid MP, Woodgett JR. FEBS Lett. 2003; 546:108. [PubMed: 12829245]
7. Alessi DR, James SR, Downes CP, Holmes AB, Gaffney PRJ, Reese CB, Cohen P. Curr Biol. 1997; 7:261. [PubMed: 9094314]
8. Sarbassov DD, Guertin DA, Ali SM, Sabatini DM. Science. 2005; 307:1098. [PubMed: 15718470]
9. Du K, Montminy M. J Biol Chem. 1998; 273:32377. [PubMed: 9829964]
10. Chung J, Grammer TC, Lemon KP, Kazlauskas A, Blenis J. Nature. 1994; 370:71. [PubMed: 8015612]
11. van Weeren PC, de Bruyn KMT, de Vries-Smits AMM, van Lint J, Burgering BMT. J Biol Chem. 1998; 273:13150. [PubMed: 9582355]
12. Zhong H, Chiles K, Feldser D, Laughner E, Hanrahan C, Georgescu MM, Simons JW, Semenza GL. Cancer Res. 2000; 60:1541. [PubMed: 10749120]
13. Li Q. Exp Opin Ther Pat. 2007; 17:1077.and references cited therein
14. Lindsley CW. Curr Top Med Chem. 2010; 10:458. [PubMed: 20180757] and references cited therein.
15. Barnett SF, Defeo-Jones D, Fu S, Hancock PJ, Haskell KM, Jones RE, Kahana JA, Kral AM, Leander K, Lee LL, Malinowski J, McAvoy EM, Nahas DD, Robinson RG, Huber HE. Biochem J. 2005; 385:399. [PubMed: 15456405]
16. Meuillet EJ, Mahadevan D, Vankayalapati H, Berggren M, Williams R, Coon A, Kozikowski AP, Powis G. Mol Cancer Therap. 2003; 2:389. [PubMed: 12700283]
17. Meuillet EJ, Ihle N, Baker AF, Gard JM, Stamper C, Williams R, Coon A, Mahadevan D, George BL, Kirkpatrick L, Powis G. Oncol Res. 2004; 14:513. [PubMed: 15559765]
18. Castillo SS, Brognard J, Petukhov PA, Zhang C, Tsurutani J, Granville CA, Li M, Jung M, West KA, Gills JG, Kozikowski AP, Dennis PA. Cancer Res. 2004; 64:2782. [PubMed: 15087394]

19. Mills SJ, Vandeput F, Trusselle MN, Safrany ST, Erneux C, Potter BVL. ChemBioChem. 2008; 9:1757. [PubMed: 18574825]
20. Huang BX, Kim HY. J Am Soc Mass Spectrom. 2009; 20:1504. [PubMed: 19446470]
21. Ropars V, Barthe P, Wang CS, Chen W, Tzou DLM, Descours A, Martin L, Noguchi M, Auguin D, Roumestand C. The Open Spectroscopy Journal. 2009; 3:65.
22. Fyrst H, Oskouian B, Bandhuvula P, Gong Y, Byun HS, Bittman R, Lee AR, Saba JD. Cancer Res. 2009; 69:9457. [PubMed: 19934323]
23. Kim D, Sun M, He L, Zhou QH, Chen J, Sun XM, Bepler G, Sebti SM, Cheng JQ. J Biol Chem. 2010; 285:8383. [PubMed: 20068047]
24. Estrada AC, Syrovets T, Pitterle K, Lunov O, Büchele B, Schimana-Pfeifer J, Schmidt T, Morad SAF, Simmet T. Mol Pharmacol. 2010; 77:378. [PubMed: 20018812]
25. Mahadevan D, Powis G, Mash EA, George B, Gokhale VM, Zhang S, Shakalya K, Du-Cuny L, Berggren M, Ali MA, Jana U, Ihle N, Moses S, Franklin C, Narayan S, Shirahatti N, Meuillet EJ. Mol Cancer Ther. 2008; 7:2621. [PubMed: 18790745]
26. Moses SA, Ali MA, Zuohe S, Du-Cuny L, Zhou LL, Lemos R, Ihle N, Skillman AG, Zhang S, Mash EA, Powis G, Meuillet EJ. Cancer Res. 2009; 69:5073. [PubMed: 19491272]
27. Meuillet EJ, Zuohe S, Lemos R, Ihle N, Kingston J, Watkins R, Moses SA, Zhang S, Du-Cuny L, Herbst R, Jacoby JJ, Zhou LL, Ahad AM, Mash EA, Kirkpatrick DL, Powis G. Mol Cancer Ther. 2010; 9:706. [PubMed: 20197390]
28. Neubert ME, Laskos SJ Jr, Griffith RF, Stahl ME, Maurer LJ. Mol Cryst Liq Cryst. 1979; 54:221.
29. Kiseleva VV, Gakh AA, Fainzil'berg AA. Izvestiya Akademii Nauk SSSR, Seriya Khimicheskaya. 1990; 9:2075.This starting material is available from ChemBridge Corporation
30. Thiel W, Mayer R. J Prakt Chem. 1990; 332:55. This starting material is available from Oakwood Products.
31. Heindl J, Schröder E, Kelm H-W. Eur J Med Chem. 1975; 10:121.This starting material is available from UkrOrgSynthesis.
32. Lee A-R, Lee H-F, Huang W-H, Chiang C-H. Zhonghua Yaoxue Zazhi. 1993; 45:115. This starting material is available from Ramidus AB.
33. Du-Cuny L, Song Z, Moses S, Powis G, Mash EA, Meuillet EJ, Zhang S. Bioorg Med Chem. 2009; 17:6983. [PubMed: 19734051]
34. GOLD [3.2]. CCDC; Cambridge, UK: 2007.
35. Warren GL, Andrews CW, Capelli AM, Clarke B, LaLonde J, Lambert MH, Lindvall M, Nevins N, Semus SF, Senger S, Tedesco G, Wall ID, Woolven JM, Peishoff CE, Head MS. J Med Chem. 2006; 49:5912. [PubMed: 17004707]
36. Tran HT, Zhang S. Manuscript in preparation.
37. Milburn CC, Deak M, Kelly SM, Price NC, Alessi DR, van Aalten DMF. Biochem J. 2003; 375:531. [PubMed: 12964941]
38. Wu WI, Voegtli WC, Sturgis HL, Dizon FP, Vigers GPA, Brandhuber BJ. Plos ONE. 2010; 5:e12913. [PubMed: 20886116]
39. Miao B, Skidan I, Yang J, Lugovskoy A, Reibarkh M, Long K, Brazell T, Durugkar KA, Maki J, Ramana CV, Schaffhausen B, Wagner G, Torchilin V, Yuan J, Degterev A. Proc Natl Acad Sci USA. 2010; 107:20126. [PubMed: 21041639]
40. Yang L, Dan HC, Sun M, Liu Q, Sun XM, Feldman RI, Hamilton AD, Polokoff M, Nicosia SV, Herlyn M, Sebti SM, Cheng JQ. Cancer Res. 2004; 64:4394. [PubMed: 15231645]
41. Barnett SF, Bilodeau MT, Lindsley CW. Curr Top Med Chem. 2005; 5:109. [PubMed: 15853641]
42. Berrie CP, Falasca M. FASEB J. 2000; 14:2618. [PubMed: 11099481]
43. Gills JJ, Castillo SS, Zhang C, Petukhov PA, Memmott RM, Hollingshead M, Warfel N, Han J, Kozikowski AP, Dennis PA. J Biol Chem. 2007; 282:27020. [PubMed: 17631503]

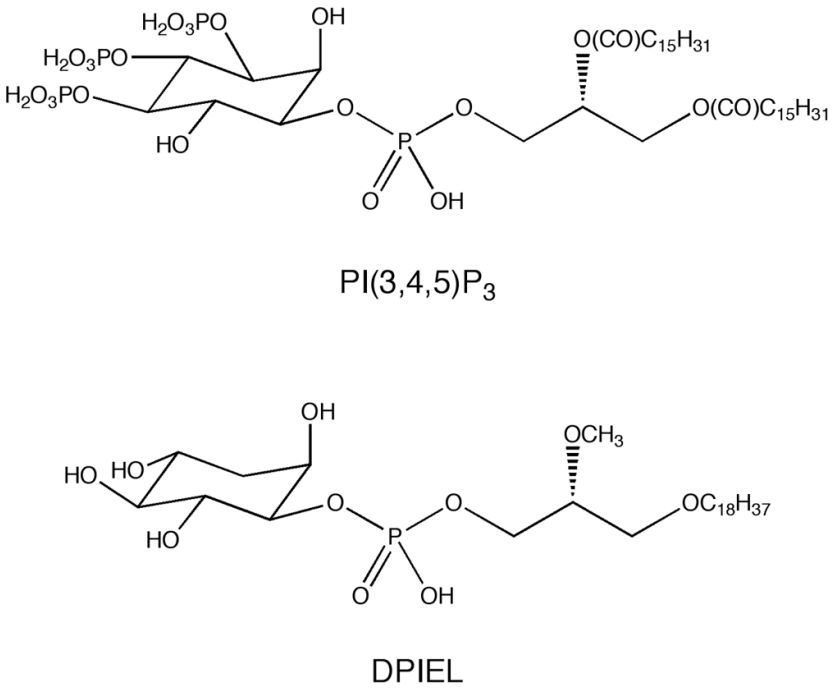

Figure 1.
The structures of PI(3,4,5)P_3 and DPIEL

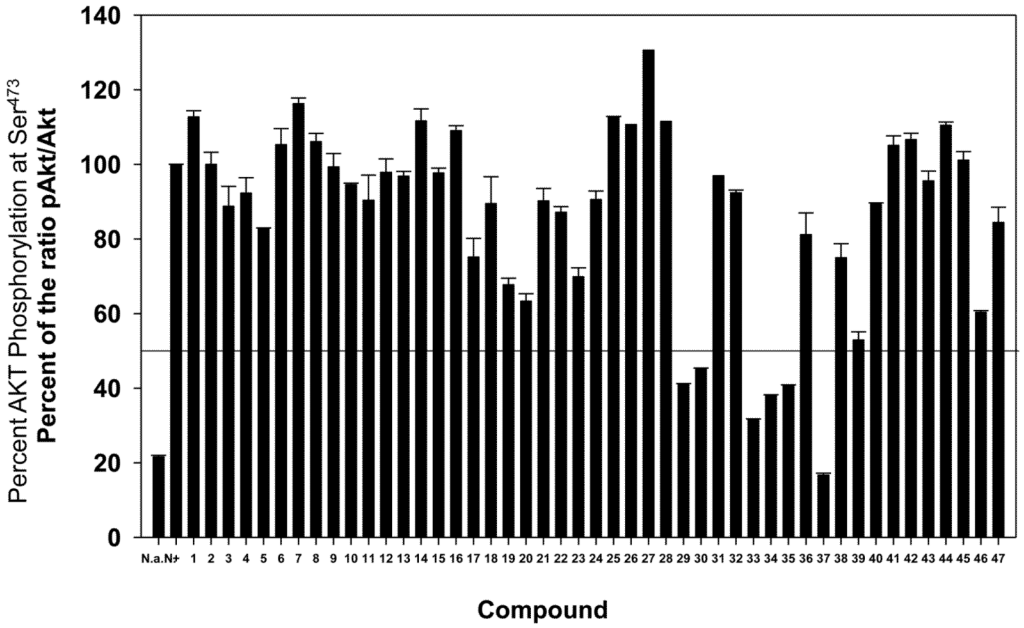

Figure 2.
Extent of AKT phosphorylation at Ser^{473} in the presence of compounds **1–47** at 10 μM.

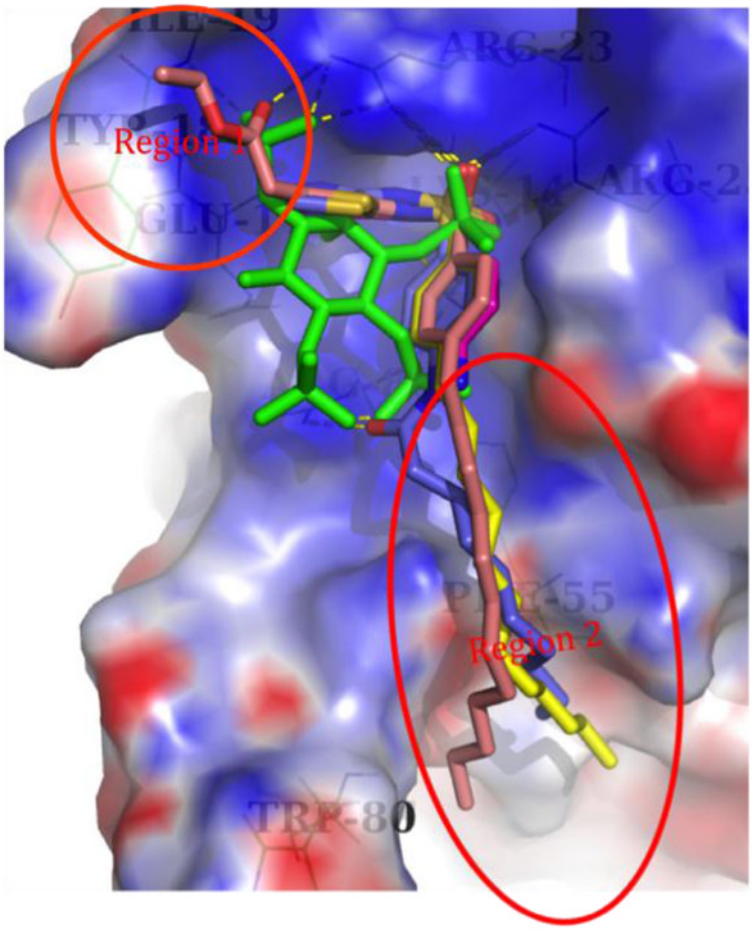

Figure 3.
The best GOLD docking poses for IP_4 (green), **1** (magenta), **17** (blue), **29** (yellow)**,** and **37** (salmon). The dashed lines represent hydrogen bonds, and the electrostatic surface is for the protein. The circled regions are those with synthetic modifications.

Figure 4.
Structural alignment of AKT kinase-PH domain (PDB code 3O96, see reference 38) and PH domain (PDB code 1UNQ, see reference 37). Blue Ribbons: 1UNQ. Green sticks: $PI(3,4,5)P_3$ from 1UNQ. Red Ribbons: 3O96. Grey sticks: inhibitor VIII from 3O96.

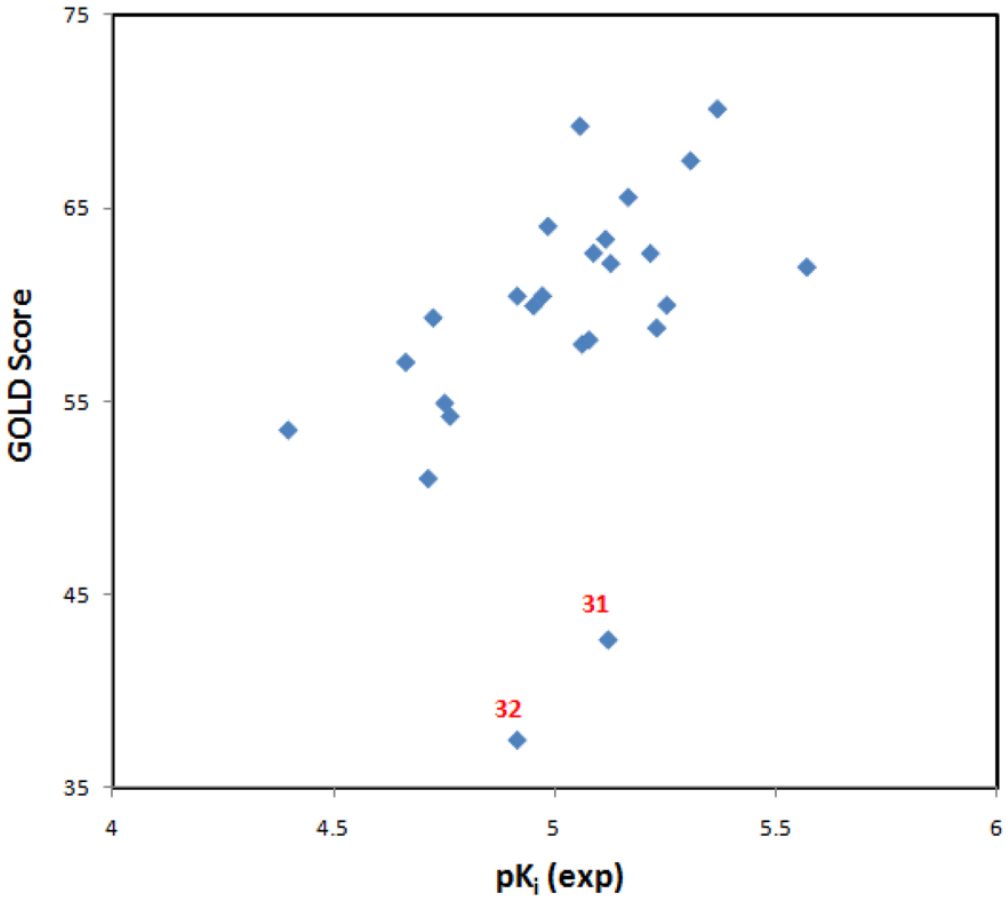

Figure 5.
The correlation between experimental pK_i values and GOLD scores. Compounds **31** and **32** are outliers, suggesting their binding mode might be different from the other compounds.

Table 1

Structures, yields, and melting points of compounds **1–47**. Details of the syntheses are given in the Experimental Section (compounds **26–40**) or in the Supplementary Data (compounds **1–25** and **41–47**).

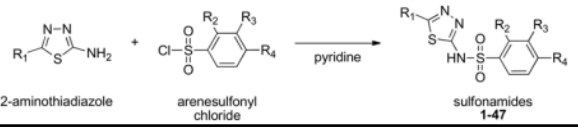

Compound	R_1	R_2	R_3	R_4	Yield (%)	mp (°C)
1[a]	H	H	H	NH_2	49[b]	224–225
2	CH_3	H	H	NH_2	72[b]	207–208
3	CH_2CH_3	H	H	NH_2	69[b]	190–191
4	$C(CH_3)_3$	H	H	NH_2	74[b]	220–221
5	CH_2CO_2H	H	H	NH_2	82[c]	209–210
6	CH_2OH	H	H	NH_2	68[b]	89–90
7	SO_2NH_2	H	H	NH_2	57[b]	241–242
8[a]	H	H	H	$NH(CO)CH_3$	95	216–217
9	CH_3	H	H	NH(CO)CH3	97	239–240
10	CH_2CH_3	H	H	$NH(CO)CH_3$	70	197–198
11	$C(CH_3)_3$	H	H	$NH(CO)CH_3$	84	137–138
12	CH_2CO_2H	H	H	$NH(CO)CH_3$	88[d]	206–207
13	$CH_2CO_2CH_2CH_3$	H	H	$NH(CO)CH_3$	76	156–157
14	$CO_2CH_2CH_3$	H	H	$NH(CO)CH_3$	73	201–202
15	CH_2OH	H	H	$NH(CO)CH_3$	82	101–102
16	SO_2NH_2	H	H	$NH(CO)CH_3$	63	280–281
17[a]	H	H	H	$NH(CO)(CH_2)_8CH_3$	95[e]	151–152
18	CH_3	H	H	$NH(CO)(CH_2)_8CH_3$	95[e]	141–142
19	CH_2CH_3	H	H	$NH(CO)(CH_2)_8CH_3$	97[e]	121–122
20	$C(CH_3)_3$	H	H	$NH(CO)(CH_2)_8CH_3$	98[e]	156–157

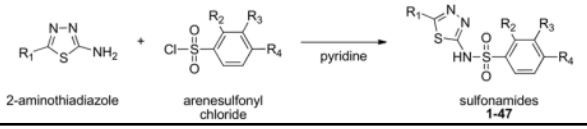

Compound	R_1	R_2	R_3	R_4	Yield (%)	mp (°C)
21	CH_2CO_2H	H	H	$NH(CO)(CH_2)_8CH_3$	83[d]	190–191
22	$CH_2CO_2CH_2CH_3$	H	H	$NH(CO)(CH_2)_8CH_3$	63	89–90
23	$CO_2CH_2CH_3$	H	H	$NH(CO)(CH_2)_8CH_3$	65	101–102
24	CH_2OH	H	H	$NH(CO)(CH_2)_8CH_3$	73	69–70
25	SO_2NH_2	H	H	$NH(CO)(CH_2)_8CH_3$	60	242–243
26	H	H	H	$(CH_2)_3CH_3$	59	120–121
27	H	H	H	$(CH_2)_5CH_3$	58	125–126
28	H	H	H	$(CH_2)_7CH_3$	55	123–124
29[a]	H	H	H	$(CH_2)_{11}CH_3$	51	126–127
30	H	H	H	$(CH_2)_{13}CH_3$	47	116–117
31	H	H	H	$(CH_2)_{15}CH_3$	46	118–119
32	H	H	H	$(CH_2)_{17}CH_3$	51	116–117
33	CH_3	H	H	$(CH_2)_{11}CH_3$	84	149–150
34	CH_2CH_3	H	H	$(CH_2)_{11}CH_3$	59	93–94
35	$C(CH_3)_3$	H	H	$(CH_2)_{11}CH_3$	87	117–118
36	CH_2CO_2H	H	H	$(CH_2)_{11}CH_3$	86[d]	194–195
37	$CH_2CO_2CH_2CH_3$	H	H	$(CH_2)_{11}CH_3$	54	110–111
38	$CO_2CH_2CH_3$	H	H	$(CH_2)_{11}CH_3$	78	134–135
39	CH_2OH	H	H	$(CH_2)_{11}CH_3$	65	138–139
40	SO_2NH_2	H	H	$(CH_2)_{11}CH_3$	63	249–250
41	H	H	H	C_6H_5	57	250–251
42	CH_2CH_3	H	H	C_6H_5	43	146–147
43	CH_2OH	H	H	C_6H_5	52	239–240
44[a]	H	H	H	$NH(CO)CH_2O(CH_2CH_2O)_2CH_3$	62	oil

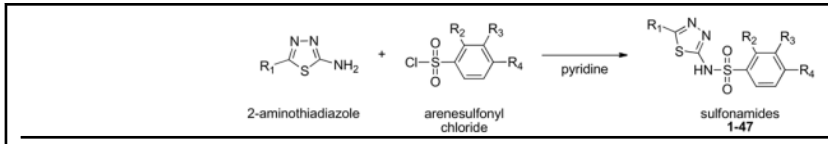

Compound	R_1	R_2	R_3	R_4	Yield (%)	mp (°C)
45	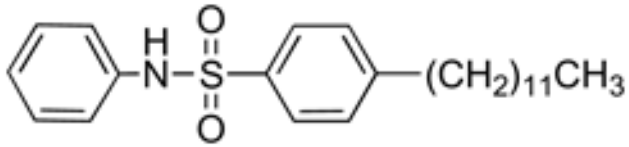				68	54–55
46	H	$(CH_2)_{11}CH_3$	H	H	13	159–161
47	H	H	$(CH_2)_{11}CH_3$	H	91	98–99

[a] Compound previously reported; see Reference 26.

[b] Yield of hydrolysis of the corresponding acetamide derivative.

[c] Yield of hydrolysis of compound **13**.

[d] Yield of hydrolysis of the corresponding ethyl ester.

[e] Yield of acylation of the corresponding aniline derivative.

Table 2

Bioassay data and GOLD docking scores for compounds **1–47**.

Compound Number	*Ki* × 10^6 (M)[a]	p*Ki*[a,b]	Cell Survival[c] *IC*50[d] (μM)	GOLD Docking Score
1	>50[e]	IA	>300	50
2	ND	ND	>300	52
3	ND	ND	>300	54
4	ND	ND	>300	55
5	ND	ND	>300	61
6	ND	ND	>300	53
7	ND	ND	>300	62
8	>50[e]	IA	>300	50
9	ND	ND	>300	51
10	ND	ND	>300	53
11	ND	ND	>300	55
12	ND	ND	>300	62
13	ND	ND	176±8	62
14	ND	ND	>300	51
15	ND	ND	>300	51
16	ND	ND	>300	57
17	22±2[e]	4.7	180±5	57
18	11±2	5.0	149±7	60
19	8±1	5.1	146±11	63
20	12±3	4.9	>300	60
21	10±2	5.0	>300	64
22	9±2	5.1	170±12	69
23	9±1	5.1	117±6	58
24	11±1	5.0	189±28	60
25	>50	IA	>300	61
26	>50[f]	IA	>300	57
27	>50[f]	IA	266±9	60
28	>50[f]	IA	100±4	57
29	2.4±0.6[e]	5.6	57±10	62
30	5.6±0.4[f]	5.2	53±8	60
31	7.6±0.3[f]	5.1	41±9	43
32	12±1[f]	4.9	39±11	38
33	>50	IA	51±14	63
34	7±1	5.2	41±1	66
35	>50	IA	41±15	66
36	5.0±0.4	5.3	117±7	68
37	4.3±0.1	5.4	63±7	70

Compound Number	$Ki \times 10^6$ (M)[a]	pKi[a,b]	Cell Survival[c] $IC50$[d] (μM)	GOLD Docking Score
38	19±2	4.7	34±3	59
39	7.5±0.6	5.1	33±3	62
40	6±1	5.2	85±9	63
41	19±2	4.7	>300	51
42	17±1	4.8	268±5	54
43	40±8	4.4	>300	54
44	41±12	4.4	>300	52
45	>50	IA	38±10	37
46	18±6	4.8	74±8	55
47	8±1	5.1	71±12	63
PI(3,4,5)P_3	0.5±0.1[f]	6.3	ND	119
DPIEL	1.6±0.2[f]	5.8	ND	40

[a] ND = not determined.

[b] IA = inactive.

[c] This assay employed BxPC3 cells.

[d] The IC_{50} is the concentration of compound required to cause 50% of the cells to die.

[e] Taken from Reference 26.

[f] Taken from Reference 27.